ELSEVIER

Journal of Nuclear Materials 258–263 (1998) 2064–2068

journal of nuclear materials

Effects of grain boundary misorientation on the solute segregation in austenitic stainless steels

T.S. Duh, J.J. Kai *, F.R. Chen, L.H. Wang

Center of Electron Microscopy, Department of Nuclear Engineering and Engineering Physics, National Tsing Hua University, 300 Hsin-chu, Taiwan, ROC

Abstract

The purpose of this study is to understand the effects of grain boundary misorientation on the solute segregation in austenitic stainless steels irradiated by protons. Many studies have shown that, for the Gibbsian type of segregation, the grain boundaries possess an ordered structure and the degree of segregation depends on the grain boundary misorientation. In contrast to the Gibbsian type of segregation, radiation induced segregation at grain boundaries is a non-equilibrium segregation phenomena. The 304 and 316L specimens were chosen for this study and irradiated by 5 MeV protons at a temperature of 450°C. The Cr/Ni-concentration profiles were measured by FEG/EDS and the grain boundary misorientation was determined by Kikuchi patterns. It seems from the preliminary results that the segregation to the grain boundary would tend to happen at boundaries with higher Σ value.

1. Introduction

Many studies have shown that the grain boundaries possess an ordered structure. The well known grain boundary structure is the dislocation model of low angle boundaries. As the misorientation angle increases, the spacing of dislocations decreases until the dislocation cores overlap and the isolated dislocation structure becomes indistinguishable. However, the resulting grain boundary structure may still be described in terms of a dense array of dislocations [1]. The degree of segregation to grain boundaries in an alloy system has been shown to be dependent upon the boundary structure [2–4]. For misorientations of small angle, small angle boundaries generally show smaller amounts of segregation than large angle boundaries in given conditions. The increase in the degree of segregation with grain boundary misorientation is attributed to the increase in lattice dislocation density with misorientation. For large angle boundaries, there is evidence that the degree of segregation is often lower at special boundaries of low energy than at general boundaries of higher energy [5].

In constrast to the Gibbsian type of segregation, radiation induced segregation at grain boundaries is a non-equilibrium segregation phenomena. In this study, we are interested in the effects of grain boundary misorientation on the radiation induced segregation in austenitic stainless steels under 5 MeV proton irradiation at elevated temperature. We used the FEG/EDS to observe the chromium/nickel-concentration profile on grain boundaries and determined the grain boundary misorientation from Kikuchi patterns. Later, in this paper we will introduce the method to determine the misorientation from Kikuchi patterns.

2. Experimental

2.1. Materials

The austenitic stainless steels were chosen because of their common use as structural materials in reactors when subjected to SCC. The chemical composition of these two materials is shown in Table 1. The as-received 316L sample was first solution annealed at 1050°C for 30

* Corresponding author. Tel.: +886 3 574 855; fax: +886 3 571 6770; e-mail: jjkai@faculty.nthu.edu.tw.

0022-3115/98/$19.00
PII: S0022-3115(98)00124-X

Table 1
Chemical composition of 304 and 316L stainless steels

	Fe	Cr	Ni	Mn	Mo	P	S	Si	N	C
304 (wt%)	bal.	18.040	8.230	1.490	0.036	0.025	0.002	0.5	0.056	0.047
316L (wt%)	bal.	15.9	10	16.1	–	0.057	0.01	0.502	–	0.02

min and furnace-cooled down to room temperature with a cooling rate 4°C/min. The 304 sample which was not solution heat treated was thermal sensitized at 650°C for 100 h and then cooled down by water quench. After heat treatment, the bulk samples were made into TEM specimens of 3 mm diameter and 80–90 μm thick for proton irradiation.

2.2. Proton irradiation

The irradiation test was performed on Tandem linear accelerator. The specimens were irradiated by protons to cause radiation-induced segregation on grain boundaries. The irradiation conditions of 316L TEM specimens are: proton beam energy is 5 MeV, average current density 21 nA/min^2, total damage dose 0.1 dpa, irradiation temperature 450°C. The 304 specimens have the same irradiation conditions as the 316L except the total dose is 0.01 dpa. The protons of 5 MeV can penetrate the specimens to a depth of 81 μm. After irradiation, the specimens were prepared by electropolishing for TEM observations.

2.3. FEG/EDS observations

The observations of grain boundary segregation and grain boundary misorientation were performed on JEOL JEM-2010F TEM with X-ray spectrometer attached to the stage. This instrument can provide a beam voltage of 200 kV and has a beam diameter of 0.5 nm. The Cr/Ni-concentration profiles near the grain boundary were measured by X-ray energy dispersive spectrometry (XEDS) and the grain boundary misorientation were observed by diffraction patterns with Kikuchi maps.

3. Results and discussion

Fig. 1 shows the typical result of this experiment. Fig. 1(a)–(c) are the Cr/Ni-concentration profile near both sides of grain boundary, the image of an edge-on grain boundary and a pair of Kikuchi patterns of the grains adjoining the boundary, respectively. Kikuchi lines are observed in the diffraction pattern if the specimen is just thick enough to generate a large number of inelastically scattered electrons.

3.1. Determination of grain boundary misorientation by Kikuchi patterns

To determine the grain boundary misorientation, first we need to know the beam direction in each grain on both sides of the boundary. A detailed procedure for determining the beam direction in grains from Kikuchi patterns has been given by Chen and King [6]. The beam direction in crystal is determined with the emulsion side up and is antiparallel to the direction of electron flow. It is possible to locate the beam spot precisely in a simulated Kikuchi pattern, as shown in Fig. 2.

The exact beam direction in each grain can then be determined by solving the relationships of beam direction $\mathbf{B}_0$ and at least three known pole directions on a simulated Kikuchi map $\mathbf{P}_1$, $\mathbf{P}_2$ and $\mathbf{P}_3$:

$$\cos(x_1/L) = \mathbf{B}_0 \cdot \mathbf{P}_1/|\mathbf{B}_0||\mathbf{P}_1|,$$
$$\cos(x_2/L) = \mathbf{B}_0 \cdot \mathbf{P}_2/|\mathbf{B}_0||\mathbf{P}_2|,$$
$$\cos(x_3/L) = \mathbf{B}_0 \cdot \mathbf{P}_3/|\mathbf{B}_0||\mathbf{P}_3|,$$

where x_1, x_2, and x_3 are the distances from beam spot in the simulated Kikuchi pattern to three known poles, respectively, and L is the camera length, provided that x/L is very small.

Next, to determine the misorientation between two grains, we can attach the Lab. frame to the photographic plate, and take the beam direction as z-axis, and the plane on the photographic plate as x–y plane. The position of the photographic plate in TEM is fixed, so is the Lab. frame. As we know, each grain has its own coordinate system. With the known beam direction and Kikuchi pattern, we can easily express the Lab. frame on photographic plate in terms of the grain coordinate system. As shown in Fig. 3, the Lab. frame in terms of coordinates of grain 1 and 2 is denoted as $\mathbf{U}_1$ and $\mathbf{U}_2$, respectively. The misorientation matrix $\mathbf{R}$ relating the two grains can be written as

$$\mathbf{R}\mathbf{U}_{1i} = \mathbf{U}_{2i}, \quad i = x,\ y \text{ and } z,$$

$$\mathbf{R}_{ij} = \mathbf{U}_{2i} \cdot \mathbf{U}_{1j}^{-1},$$

where $\mathbf{R}$ is a 3×3 matrix, $\mathbf{R}_{ij}$ is the element of matrix $\mathbf{R}$, and $\mathbf{U}_{1i}$ and $\mathbf{U}_{2i}$ are column vectors. The orientation relationship between two grains can be described by rotation about an axis. The rotation axis is given by the unit vector parallel to

$$[\mathbf{R}_{32} - \mathbf{R}_{23}, \mathbf{R}_{13} - \mathbf{R}_{31}, \mathbf{R}_{21} - \mathbf{R}_{12}]$$

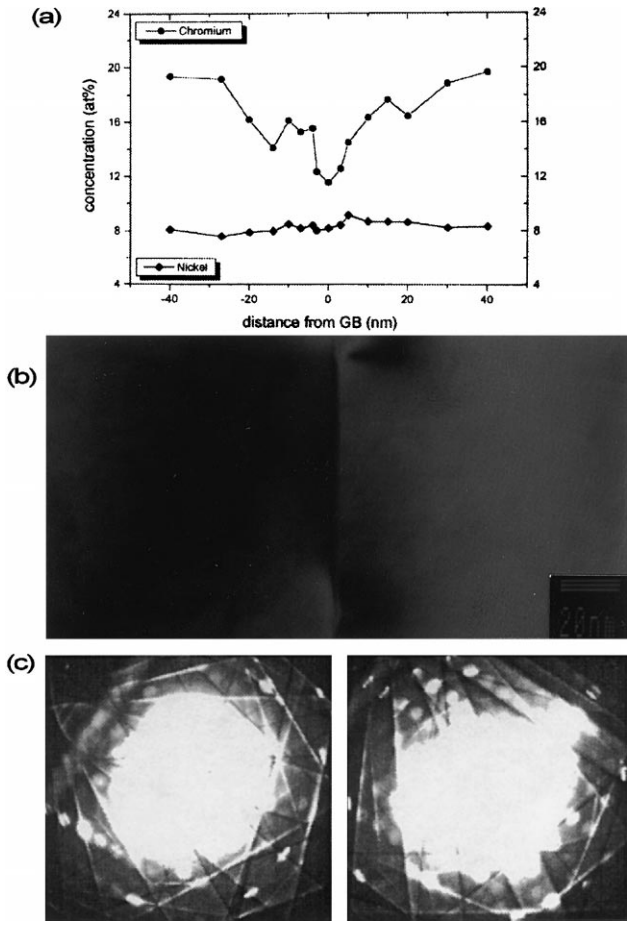

Fig. 1. (a) Cr/Ni-concentration profile near grain boundary; (b) the image of grain boundary; (c) a pair of Kikuchi patterns of the grains adjoining the boundary.

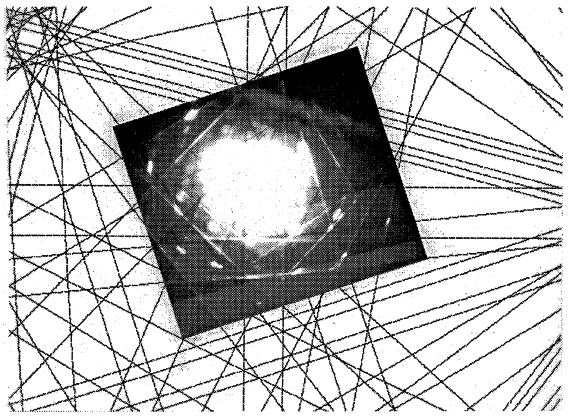

Fig. 2. A good match between the measured and simulated Kikuchi patterns. The measured Kikuchi pattern is shown in the central part.

and the rotation angle θ by
$\theta = \cos^{-1}((\mathbf{R}_{11} + \mathbf{R}_{22} + \mathbf{R}_{33} - 1)/2)$.

With the rotation axis and angle, the corresponding Σ value can be found from the table made by Mykura in which are listed values of rotation axis and angle for CSL's up to Σ101 [7].

3.2. Grain boundary segregation vs. misorientation

The degree of Cr-depletion at grain boundary vs. grain boundary misorientation is shown in Table 2. We can see in Table 2 that the measured grain boundary misorientations are not exact CSL orientations. They all depart from CSL orientations by $\Delta\theta$ (rotation angle shift) and ΔZ (rotation axis shift), and this usually happens in polycrystalline metals and alloys [8]. In Table 2, we can see that some of the grain boundaries have Cr-depletion, and some do not. Nickel enrichment at grain boundary was not clearly observed. From the present study, it seems that the Cr-depletion would tend to happen at boundaries with higher Σ value, and that the degree of Cr-depletion at grain boundaries would

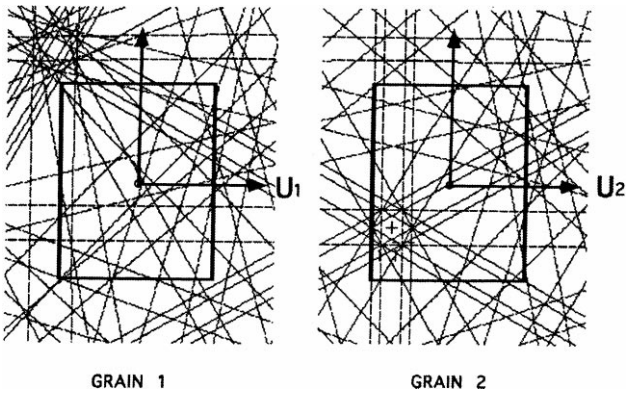

Fig. 3. A pair of Kikuchi patterns with photographic plate attached. The Lab. Frame on the plate can be expressed in terms of coordinates of grain 1 and 2 and is denoted as $\mathbf{U}_1$ and $\mathbf{U}_2$, respectively. $\mathbf{U}_1$ and $\mathbf{U}_2$ are relating by misorientation matrix $\mathbf{R}$, $\mathbf{R}\mathbf{U}_1 = \mathbf{U}_2$.

Table 2
Grain boundary segregation vs. misorientation

Specimen	Σ	Axis	Angle°	$\Delta\theta$°	ΔZ°	Cr-depletion depth
304, 0.01 dpa, 450°C	37	[0,1,0]	18.92	0.28	6.4	8%
	37	[2,1,4]	97.75	4.73	1.63	6%
	1		2.6			No
	33	[1,1,0]	121.02	5.17	7.7	No
316L, 0.1 dpa, 450°C	35	[−1,1,2]	122.89	0.96	3.8	3%
	7	[−1,−1,2]	135.58	1.98	2.51	No
	1		9.6			No
	23	[2,5,1]	107.72	7.49	1.43	No

depend upon boundary structure. We need more data to validate this.

There is evidence of other works that the degree of segregation to grain boundaries depends on boundary structure. As shown in Fig. 4(a), Watanabe [2] found that, in his study on the effect of boundary misorientation on grain boundary segregation of tin in iron–tin alloy, the amount of tin segregation increases rapidly in the low angle region and then shows a cusp around 70° which corresponds to $\Sigma 3$ coincidence misorientation relationship. In Fig. 4(b), measurements of grain boundary free energy σ as a function of tilt angle θ are shown. We can also see that there is an energy cusp at $\Sigma 3$ boundary [5]. From the classical Gibbs expression,

$$\Delta N = -(X/kT)\ \mathrm{d}\sigma/\mathrm{d}X,$$

where ΔN is the grain boundary excess, X is the solute concentration in matrix, we can see that the grain boundary segregation is relating to the free energy, σ, of the boundary. In the study on grain boundary diffusion by Lange and Jurisch [9], the measurements of grain boundary diffusion coefficient of aluminum as a function of tilt angle are shown in Fig. 4(c). There is also a cusp observed near $\Sigma 3$. The schematic diagram of the usual path for solute segregating to grain boundaries is shown in Fig. 5 [10]. Most of the solutes segregating to grain boundary touch the boundary surface first, then diffuse to grain boundary dislocations through grain boundary and then to jog sites. The grain boundary diffusion may play a role in grain boundary segregation. The $\Sigma 3$ {1 1 1} is a twin boundary of relatively low energy and contains few sites for attracting solute atoms. From the evidence described above, for small misorientation, small angle boundaries generally show smaller amounts of segregation than large angle boundaries in given conditions. For large angle boundaries, the degree of segregation is often lower at special boundaries of low energy than at general boundaries of higher energy.

4. Summary

The results of this study are summarized as follows:

1. The irradiated 304 and 316L specimens were observed by FEG/EDS and the Cr-depletion was observed only at some of the grain boundaries.
2. The grain boundary misorientation was determined by Kikuchi pattern analysis.

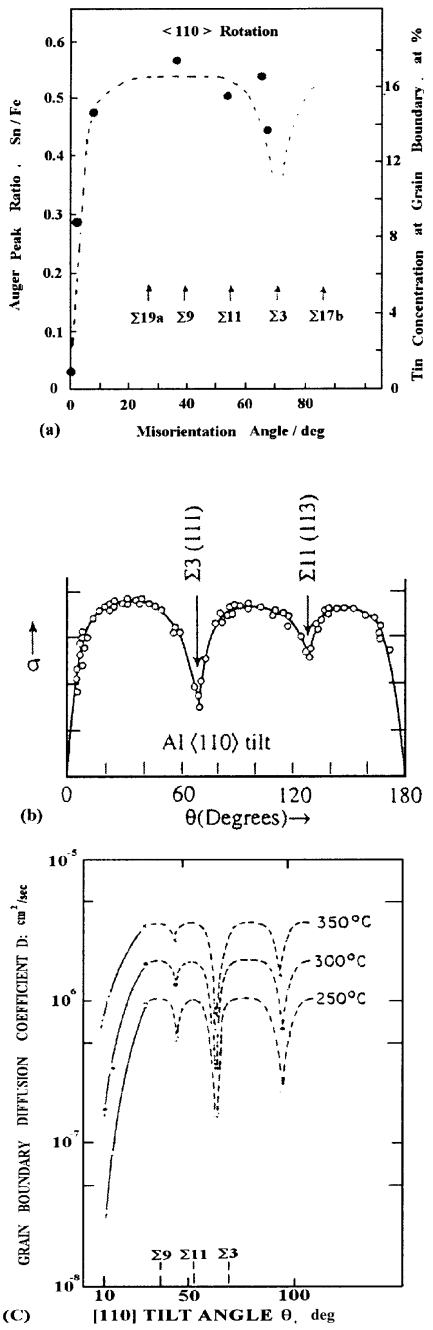

Fig. 4. (a) Misorientation dependence of tin segregation as a function of rotation angle about ⟨1 1 0⟩ axis in α-Fe – 1.08 at.% tin alloy [2]. (b) Measured variation σ with tilt angle, θ, for ⟨1 1 0⟩ Symmetric tilt grain boundaries in Al [5]. (c) Grain boundary diffusion coefficient in [1 1 0] tilt boundaries of Al as a function of misorientation angle [9].

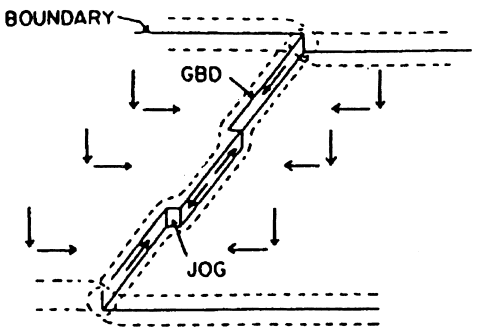

Fig. 5. The usual way for solute segregating to grain boundary is indicated by arrows. Most of the solutes segregating to grain boundary touch the boundary surface first, then diffuse to grain boundary dislocations through grain boundary and then jog sites [10].

3. It seems from the preliminary results that segregation to grain boundaries is more likely at boundaries with higher Σ value.

Acknowledgements

This study is supported by National Tsing Huna University Center of Electron Microscopy, Van de Graaff Accelerator Center and Tandem accelerator for proton irradiation.

References

[1] W.T. Read, W. Shockley, Phys. Rev. 78 (1950) 275.
[2] T. Watanabe, J. Phys. (Paris) Colloq. C4 46 (Suppl. 4) (1985) c4-555.
[3] A. Seki, D.N. Seidman, Y. Oh, S.M. Foiles, Acta Metall. 39 (1991) 3179.
[4] T. Ogura, C.J. McMahon, H.C. Feng, V. Vitek, Acta Metall. 26 (1978) 1317.
[5] A.P. Sutton, R.W. Balluffi, Interfaces in Crystalline Materials, Clarendon, Oxford, 1996.
[6] F.R. Chen, A.H. King, J. Electron Microscopy Techn. 6 (1987) 55.
[7] H. Mykura, Grain Boundary Structure and Kinetics, American Society for Metals, Metals Park, OH, 1980, p. 445.
[8] C.T. Forwood, L.M. Clarebrough, Electron Microscopy of Interfaces in Metals and Alloys, Adam Hilger, New York, 1991, p. 134.
[9] W. Lange, M. Jurisch, quoted in H. Gleiter, B. Chalmers, Prog. Mater. Sci. 16 (1972).
[10] R.W. Balluffi, A.H. King, Phase Transformations during Irradiation, Applied Science, Barking, 1983, p. 147.